J. COMBIN. MATH. COMBIN. COMPUT. 127a (2025) 5591--5614

Journal of Combinatorial Mathematics and Combinatorial Computing
www.combinatorialpress.com/jcmcc

Combinatorial Press

Fourier transform-based pattern design method and geometric deformation in lacquer decorative design

Jing Wang[1,✉]

[1] *Sichuan Vocational and Technical College of Communications, Chengdu, Sichuan, 611130, China*

ABSTRACT
In order to optimize the pattern design method in lacquerware decoration design, this paper first analyzes the discrete and continuous situation of the pattern in time and frequency by Fourier transform method, and explains the mapping principle of Fourier variation. After that, the original image is processed such as sharpening and smoothing under the Fourier transform algorithm, and the lacquer decorative pattern after automatic deformation is obtained through interaction on the basis of 2D affine transformation technology. Finally, the geometric deformation of the lacquer decoration design from 2D to 3D is simulated and verified. The results show that in this paper, the threshold value, brightness and contrast of the lacquer decorative design patterns can be obtained by the geodesic distance deformation algorithm under the Fourier transform in MATLAB software to get the geometric patterns of the lacquer decorative design with the main color of the appropriate filler blocks. The corresponding blue values of the four patterns are 418, 38, 104 and 256; the optimal values of green are 256, 100, 87 and 405; and the optimal values of red are 256, 57, 63 and 117. 3-D imaging simulation experiments show that the average absolute error, root mean square error and maximum absolute error of the depth of the geometric patterns of the 3-D imaging method and the geometric patterns proposed in this paper are all significantly reduced, and the depth of the geometric patterns in the 20-mm depth range are reduced significantly. and the advantages of this paper's method are more obvious in the depth variation range of 20mm. It can be seen that the algorithm of this paper can improve the deformation effect of geometric patterns in lacquer decorative design.

Keywords: Fourier transform, 2D affine transform, geodesic distance deformation algorithm, lacquer decoration

1. Introduction

In terms of the current stage of development, Chinese art has a history of thousands of years. Decorative art has been born as early as the primitive society period, through all kinds of different

✉ Corresponding author.
E-mail address: wangjing123mm@163.com (J. Wang).
Received 25 February 2024; Revised 10 May 2024; Accepted 15 December 2024; Published Online 15 April 2025.
DOI: 10.61091/jcmcc127a-312
© 2025 The Author(s). Published by Combinatorial Press. This is an open access article under the CC BY license (https://creativecommons.org/licenses/by/4.0/).

color patterns for display, so as to express different thoughts and emotions [1-2]. With the continuous progress of science and technology and economy, the development of lacquerware products is gradually becoming one of the production and consumption objects that China attaches great importance to. Nowadays, because of the combination of decoration and craftsmanship, lacquer products have been widely loved by people [3]. From the point of view of art appreciation, lacquerware products have a unique sense of rhythm and rhythm, not only has the beauty of image, but also has the abstract beauty [4-5]. For the creators, in order to be able to express their inner theme and emotional value, they should make an article in the craft level, choose the right material, so as to show a more perfect effect [6-8].

Generally speaking, the design style of lacquer decoration pays more attention to the beauty of form, that is, the plane, three-dimensional and color composition, so as to break the limitations of the original time level and space level, through the reasonable setup and division, so as to form a unique sense of beauty [9-12]. Relying on different types of contrast, to promote a certain sense of rhythm and rhyme [13-14]. In order to fully express their own ideas and intentions, the creators must think about how to choose the most appropriate materials and forms, in order to be able to achieve the actual creation of the actual plan [15-16]. With the development of digital technology, the method of lacquer pattern design has also ushered in major changes.

In this paper, the case of continuity and dispersion of Fourier transform is illustrated in time and frequency to get the spectrogram of lacquer decorative patterns. In MATLAB, some simple point and line patterns provided by the system are selected and combined to obtain the base pattern. Decompose the base pattern to get a new pair of color patterns as the final design result output. Select a number of points on the image as a control set and specify the corresponding target position, and then combine the use of interactive methods to obtain the automatically deformed image. The effect of geometric deformation from 2D image to 3D image in lacquer decorative design is optimized by segmenting the image and color extraction. Finally, the application effect of the algorithm in this paper is verified by 3D imaging simulation experiments.

2. Fourier transform-based patterning methods

2.1. Fourier transform

Fourier transforms [17] can be categorized into four types according to the combination of discrete and continuous cases in time and frequency, Fourier transforms are shown in Table 1. In the time and frequency domains, continuous on one of the domains represents non-periodic on the other, while the opposite is true for discrete on one of the domains represents periodic on the other and vice versa. Each Fourier transform has a corresponding Fourier inverse transform that represents the process by which images are transformed into each other between the frequency and spatial domains.

Table 1. Fourier transform

Time	frequency	transformation	symbol
Continuous nonperiodic	Continuous nonperiodic	Fourier transform	FT
Continuous period	Discrete nonperiodic	Fourier series	FS
Discrete nonperiodic	Continuous period	Discrete time Fourier transform	DTFT
Discrete period	Discrete period	Discrete Fourier transform	DTF

The Fourier domain, which can also be referred to as the frequency domain, corresponds to the time domain. The time domain is the real image that describes the change of a signal over time, however the frequency domain shows the invariance of time. The two-dimensional image described in this paper is also referred to as the spatial domain, which has the same characteristics as the time domain. In practice, the frequency domain is usually represented using a spectrum for ease of analysis and understanding. The spectrum can also be referred to as the amplitude spectrum in terms of formation and is independent of the phase of the wave. A spectrum is a picture of frequency and amplitude. A one-dimensional spectrum studies a sinusoidal wave, whose horizontal and vertical coordinates represent the frequency and amplitude, respectively. The two-dimensional spectrum is a complex plane wave, in which the frequency of coordinate point (a,b) is equal to its distance from the center zero point $\sqrt{a^2+b^2}$, the magnitude of amplitude is the value of the point, and the direction of the wave is the direction of vector (a,b). A two-dimensional plane wave can be represented by a complex number of the form $a+bi$, with $i^2=-1$ being the complex unit. The phase φ of the wave is $\arctan(b/a)$ and the amplitude R is $\sqrt{a^2+b^2}$. Figure 1 shows a point on the unit circle in the complex plane.

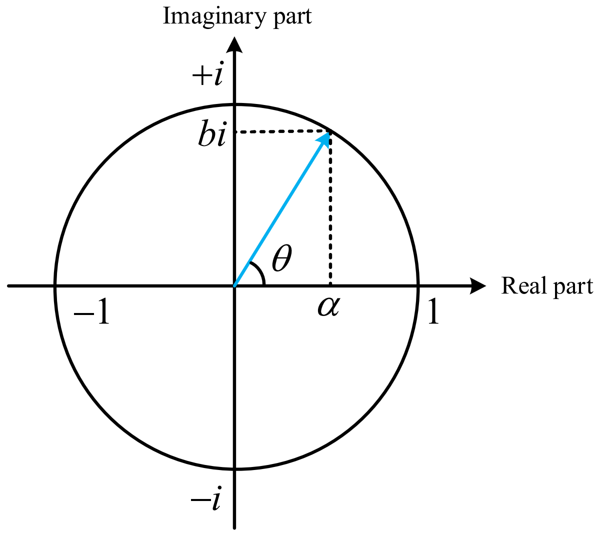

Fig. 1. Unit complex plane wave

Before describing the Fourier transform formula, the space domain and frequency domain symbols that are often used in the formula are first listed. f is a periodic function in the two-dimensional plane, and $\vec{a}$ and $\vec{b}$ are the translational period vectors of the function in both directions, that is, the basis vectors of the Bravais lattice, which can form a parallelogram region. $(\vec{a},\vec{b})$ and $(\vec{u},\vec{v})$ are a pair of related mutually inverse basis vectors, and from $\vec{a}$ and $\vec{b}$ the values of the dyadic lattice basis vectors $\vec{u}$ and $\vec{v}$ can be obtained by calculation. The two lattices of the reciprocal lattice need to satisfy that the multiplication between any two vectors belonging to different lattices must be an integer, which is defined in the plane symmetry group to be an integer multiple of 2π, and thus the relationship between them can be expressed as follows:

$$\vec{a}\cdot\vec{v}=\vec{b}\cdot\vec{u}=0\,,\vec{a}\cdot\vec{u}=\vec{b}\cdot\vec{v}=2\pi \tag{1}$$

Base vector - $(\overrightarrow{e_x},\overrightarrow{e_y})$ - $(\overrightarrow{e_x},\overrightarrow{e_y})$.

Translate the basis vectors-- $(\vec{a},\vec{b})$ -- $(\vec{u},\vec{v})$.

Coordinates under the basis vectors -- (x,y) -- (s_x,s_y).

Vectors-- $\vec{r}$ -- $\vec{s}$.

Vectors with parameters -- $\vec{r}(x,y)=x\overrightarrow{e_x}+y\overrightarrow{e_y}$ -- $\vec{s}(g,h)=g\vec{u}+h\vec{v}$.

Vector formulas-- $f(\vec{r})$ -- $F(\vec{s})$.

The value of coordinate point $\vec{r}(x,y)$ in the spatial domain is $f(\vec{r})=f(x,y)$, which can be expressed in terms of basis vectors $\vec{e}_x=(0,1)$ and $\vec{e}_y=(1,0)$ as $(x,y)=\overrightarrow{xe_x}+\overrightarrow{ye_y}$. The point in the frequency domain under the translational basis vectors is expressed as $\vec{s}(g,h) = g\vec{u} + \overrightarrow{hv}$ which is equivalent to the point $(s_x, s_y) = s_x\overrightarrow{e_x} + s_y\overrightarrow{e_y}$ expressed under the basis coordinate vectors, which has a value of $F(s) = F(g,h)$ in terms of frequency.

The Fourier transform formula converts the space domain to the frequency domain, and its time domain integral (continuous) form can be expressed as:

$$F_{\vec{s}} = \frac{1}{\Omega}\int_{\Omega} f(\vec{r})e^{-i\vec{s}\cdot\vec{r}}d\vec{r} \tag{2}$$

where Ω is the area of the parallelogram enclosed by vectors $\vec{a}$ and $\vec{b}$ and i is the complex unit.

The DFT is a realization of the Fourier transform over a set of discrete time-domain frequencies, whose spatial-domain waveforms are obtained by sampling discrete times over a finite time interval. The summation (discrete) form of the DFT formula can be expressed as:

$$\begin{gathered} F(u,v) = \frac{1}{MN}\sum_{x=0}^{M-1}\left[\sum_{y=0}^{N-1} f(x,y)W_N^{vy}\right]W_M^{ux} \\ u = 0,1,\ldots,M-1; v = 0,1,\ldots,N-1 \end{gathered} \tag{3}$$

where $M \times N$ is the number of points sampled in the two-dimensional spatial region and W_n^j is the j rd n-equivalent point on the complex unit circle.

From Euler's formula:

$$W_n^j = e^{\frac{-2\pi j}{n}} = \cos\frac{-2\pi j}{n} - i\sin\frac{-2\pi j}{n} \tag{4}$$

The Fourier results obtained on the theoretical derivation are based on the integral Fourier transform, but in practice the summation Fourier transform is used.

The two-dimensional frequency domain inverse Fourier transform formula is expressed as:

$$f(\vec{r}) = \sum_{g=-\infty}^{+\infty}\sum_{h=-\infty}^{+\infty} F_{\vec{s}(g,h)}e^{i\vec{s}(g,h)\cdot\vec{r}} \tag{5}$$

Fast Fourier Transform FFT is used on the computer to speed up the computation of the DFT results by recursive partitioning to reduce the computation of $O(N^2)$ to $O(NlogN)$. The spectrogram of the 2D image is the result of one DFT done on each of the 2D spatial data in two directions on the x and y axes, respectively, and the sequence of the two computations does not have an effect on the results.

2.2. *Principles of plotting Fourier variations*

Fourier transform is mainly used in signal analysis, Fourier transform can simplify the complex signals, that is, it can be an infinite number of different frequencies of the sine or cosine signal synthesis of a specified periodic signal, and vice versa, the Fourier transform can be a simple signal complexity, that is, a periodic function is decomposed into a finite or infinite number of different frequencies of the sine or cosine signal of the weighting. And because of the periodicity of the trigonometric series, it is foreseen that the geometries obtained by using the output of the Fourier transform will have a periodic rhythmic rhythm.

In MATLAB, some simple point and line patterns provided by the system are selected and combined to obtain a base pattern with width m and height n. The base pattern is then converted to a base pattern with width m and height n. The system internally understands this base pattern as an image signal, which is decomposed into a matrix, the elements of which represent the pixels in the image, defined as a two-dimensional function f(m, n). The discrete Fourier transform DFT of the two-dimensional image is programmed to obtain F(p, q), i.e., these simple point and line signals are decomposed into an accumulation of sinusoidal signals, and the amplitude of these sinusoidal signals |F(p, q)- is extracted. In order to bring out the details of the part of |F(p, q)- close to the value of 0, a logarithmic transformation is used, i.e., log(|F(p, q)-+1) is used for this display. After discrete Fourier inverse transform IDFT the result is redefined as a new image. Based on this the HSV color model is then used to define the color characteristics such as hue, saturation and brightness of each point. There are 2 schemes for defining color information in this study: one is an incompletely controllable scheme, i.e., the designer specifies the color types, and the computer randomly takes several of them for color distribution: the other is a completely controllable scheme, i.e., the designer controls the color information of each point by specifying the color mixing step and the fixed color taking value. Finally, a new color pattern is obtained, which is output as the final design result.

2.3. Converting True Color Images to Grayscale Images

To convert a true color image to a grayscale image [18], the grayscale value of each pixel point can be set:

$$f(i,j)=(R+G+B)/3 \tag{6}$$

In the above equation, R, G, and B are the color component values of red, green, and blue of the pixel points in the true color image, respectively.
1) Fourier positive and inverse transforms of the image. For a unitary function $f(x)$, we define a one-dimensional Fourier positive transform:

$$F(s)=\int_{-\infty}^{\infty} f(x)e^{-2\pi jsx}d(x) \tag{7}$$

Its inverse conversion:

$$f(x)=\int_{-\infty}^{\infty} f(s)e^{2\pi jsx}d(s) \tag{8}$$

Here let $j^2=-1$ be set;
For a one-dimensional discrete function $f(x)(x=0,1,2,...,N-1)$, its Fourier positive transform can be written as:

$$F(u)=\frac{1}{N}\sum_{x=0}^{N\text{-}1} f(x)e^{\text{-}j2\pi\frac{u}{N^x}} \quad (u=0,1,2,\cdots,N\text{-}1) \tag{9}$$

Its Fourier inverse transform is:

$$f(x)=\sum_{u=0}^{N-1}F(u)e^{j2\pi\frac{x}{N}u} \quad (x=0,1,2,\cdots,N-1) \tag{10}$$

For a binary function $f(x,y)$ with a two-dimensional Fourier positive transform:

$$F(u,v)=\int_{-\infty}^{\infty}\int_{-\infty}^{\infty} f(x,y)e^{-}j2\pi(ux+vy)dxdy \tag{11}$$

Its inverse transformation is:

$$f(x,y)=\int_{-\infty}^{\infty}\int_{-\infty}^{\infty} F(u,v)e^{j}2\pi(ux+vy)dudv \tag{12}$$

In digital image processing, the pixel points are two-dimensional discrete, for an image $f(x,y)$, let the image size be $M\times N$ pixel points (M is the height of the image, N is the length of the image), i.e., $x=0,1,...,M-1, y=0,1,...,N-1$, the image can be represented as a two-dimensional sequence of discrete points, which is expressed by the following equation:

$$f(x,y)=\begin{bmatrix} f(0,0) & f(0,1) & \cdots & f(0,N-1) \\ f(1,0) & f(1,1) & \cdots & f(1,N-1) \\ \cdots & \cdots & \cdots & \cdots \\ f(M-1,0) & f(M-1,1) & \cdots & f(M-1,N-1) \end{bmatrix} \tag{13}$$

For pixel $f(x,y)$ of the image, its 2D discrete Fourier positive transform can be written as:

$$F(m,n)=\frac{1}{MN}\sum_{y=0}^{M+1}\sum_{x=0}^{N-1} f(x,y)e^{-j2\pi(my+nx)} \\ (m=0,1,\cdots,M-1; y=0,1,\cdots,N-1) \tag{14}$$

Its inverse transformation is:

$$f(x,y)=\sum_{m}=0^{N+1}\sum_{n=0}^{N+1}F(m,n)e^{j}2\pi(m\frac{y}{m}+n\frac{x}{T}) \tag{15}$$

Here m,n is set as the frequency variable where $x=0,1,2,...,N-1$; $y=0,1,2,...,M^{-1}$.
2) Inverting the gray value for inverse transformation. In order to realize the sketching effect, the gray value of each point can be inverted, the original gray value of the pixel point is $f(x,y)$, and the new gray value of the point is $f(x,y)=255-f(x,y)$ by inverting the inverse transformation. In this way, the new gray value of each point can be calculated row by row and column by column.
3) Sharpening the image. Image contour region there is a more obvious gray-scale difference, the discrete second-order difference method can be used to sharpen the processing.

Remember that the original gray value of the pixel point is $f(i,j)$ and the discrete second-order differencing is $\nabla^2 f(i,j)=\nabla_x^2 f(i,j)+\nabla_y^2 f(i,j)$, i.e., the new gray value is:

$$f(i,j)=[f(i+1,j)+f(i-1,j)+f(i,j+1)+f(i,j-1)]-4f(i,j) \tag{16}$$

The enhancement of the edge contours in the image can be realized by applying the above processing to each pixel point of the image.

4) Smoothing the image. The gray value of each point, the sketch effect of the image can be realized. We use local averaging method. Let the gray value of a pixel in the image be $f(i,j)$, its neighborhood S is a square window of $N\times N$, and the total number of points in the set of points in the window is M, then the new gray value of the point after smoothing by the local averaging method is:

$$f(i,j)=\frac{1}{M}\sum_{i,jS} f(i,j) \tag{17}$$

We take $N=3, M=9$, then:

$$f(i,j)=\frac{1}{9}\sum_{i,j\le 3} f(i,j)=[f(i-1,j-1)+f(i-1,j)+f(i-1,j+1)+f(i,j-1) \\ +f(i,j)+f(i,j+1)+f(i+1,j-1)+f(i+1,j)+f(i+1,j+1)]/9 \tag{18}$$

2.4. Geometric deformation algorithm for lacquer pattern based on geodesic distance

2.4.1. 2D affine transformations:

1) The basic knowledge of affine transformations. Parallel projection [19]: in the same plane, line L and line a,a' are not parallel, perspective affine schematic shown in Figure 2, over the line a on the point $A,B,C,D,\cdots$ were made L of the parallel line, and a' of the intersection of $A',B',C',D',\cdots$ such a one-to-one relationship is called line a and a' between the perspective affine or parallel projection.

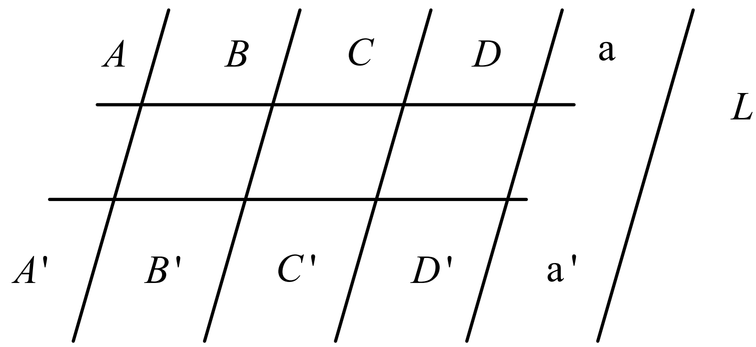

Fig. 2. Schematic diagram of perspective affine

Affine: Suppose there are several straight lines $a_1, a_2, \cdots a_n$ in the same plane, the affine schematic shown in Figure 3. Use $T_1, T_2, \cdots T_{n-1}$ to denote the perspective affine of a_1 to a_2, a_2 to a_3, a_{n-1} to a_n, respectively, after this series of parallel projections, the point on a_1 and the point on a_n to establish a one-to-one correspondence, known as the affine of a_1 to a_n or affine counterpart, notated as T, and then $T = T_{n-1}T_{n-2}\cdots T_1$ is known as the product of $T_1, T_2, \cdots T_{n-1}$, i.e., the affine is composed by the product of a finite number of parallel projections, so the affine is a chain of perspective affine or a chain of parallel projections.

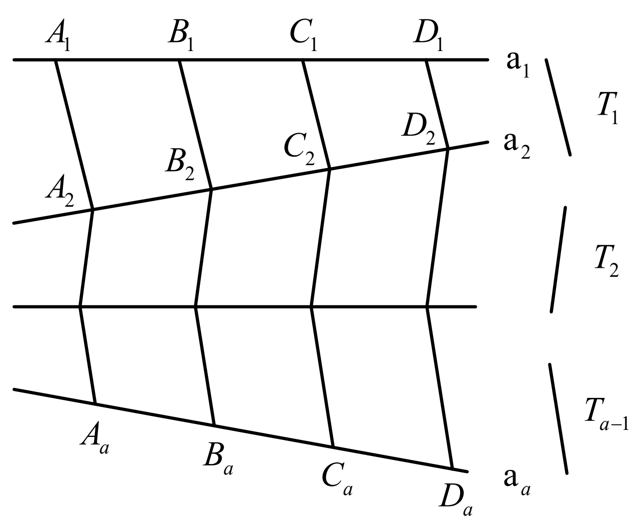

Fig. 3. Schematic diagram of affine

Parallel projections between two planes: parallel projections or perspective affinities T of two planes π to π'. The direction of the parallel projections L requires that they be neither parallel to π nor to π'. Similarly, the direction of the projection determines the perspective affine from π to π'. If $T(A) = A', T(B) = B', T(C) = C'$, and A, B, C are co-linear, it is easy to see that A', B', C' is also co-linear. Let a denote the line ABC, and a' denote the line $A'B'C'$, then write $T(a) = a'$, and the schematic diagram of the point and line union properties is shown in Fig. 4. Parallel projections between two planes have this property:

Property 1: The geometrical elements remain of the same kind without change under correspondence.

Property 2: Perspective affine retains the corresponding point on the corresponding line.

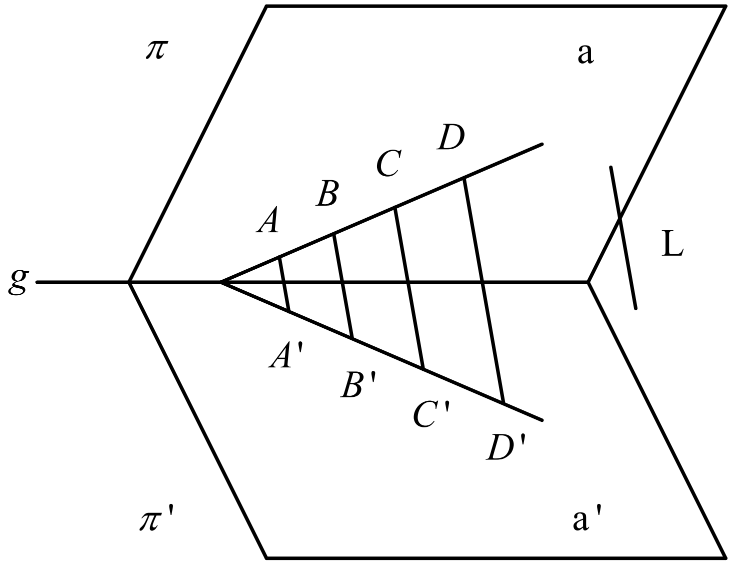

Fig. 4. Schematic diagram of the articulation of points and lines

2) Algebraic representation of affine transformations. Given a Cartesian coordinate system Oxy in the plane π, Cartesian coordinates in the plane π are shown in Fig. 5, E is the unit point, E has the coordinates (1, 1), then the coordinates (x, y) of any point p in π can be expressed as $x = \frac{OP_x}{OE_x}, y = \frac{OP_y}{OE_y}$. Here, points E_x and E_y are projections of point E on the xth and yth axes parallel to the yth and xth axes, respectively, which are called unit points of the xth and yth axes, and P_x, P_y is a projection of point P on the xst and ynd axes parallel to the yrd and xth axes, respectively.

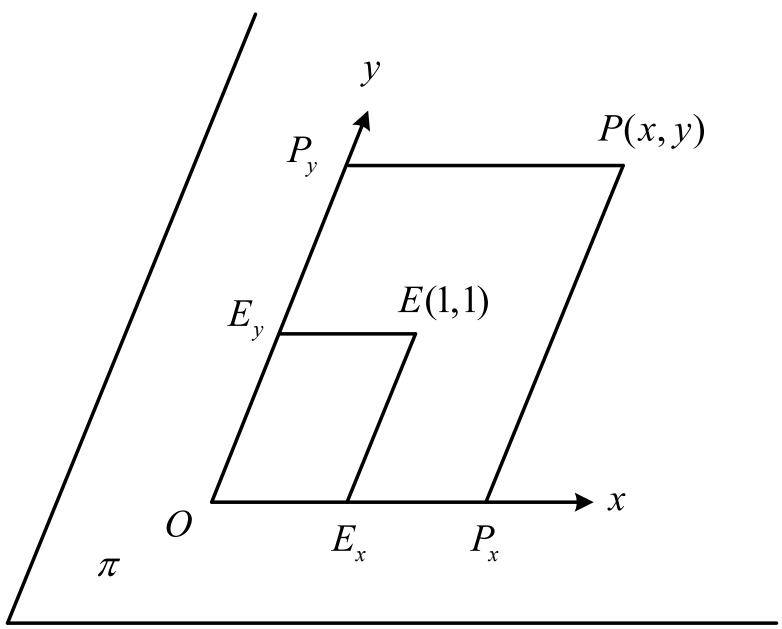

Fig. 5. Cartesian coordinate system Oxy in the plane π

Consider the affine counterpart of the graph of coordinate system Oxy in another plane π'. The Cartesian coordinates on plane π' are shown in Fig. 6. Let the images of Ox, Oy, E, P be $O'x', O'y', E', P'$ respectively, so that the images of parallelogram OE_xEE_y, OP_xPP_y are parallelograms $O'E_x'E'E_y', O'P_x'P'P_y'$ respectively.

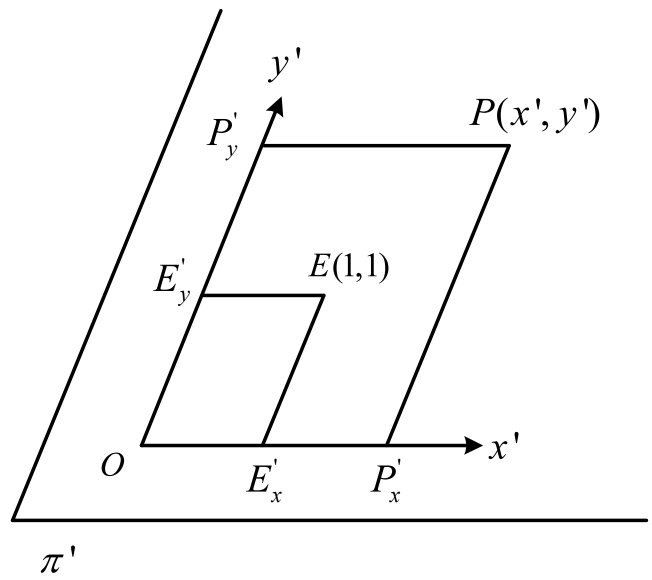

Fig. 6. Cartesian coordinate system O'x'y on the plane π'

Treat point E' as the unit point in the new coordinate system $O'x'y'$, that is, use the directed line segment $\overline{O'E_x'}, \overline{O'E_y'}$ as the unit of measurement for axis $O'x', O'y'$. For this coordinate system, the coordinate (x', y') of point P' can be expressed as $x' = \frac{O'P_x'}{O'E_x'}, y' = \frac{O'P_y'}{O'E_y'}$, and since the affine counterpart keeps the simple ratio constant, there is $x' = x, y' = y$.

Assuming that the coordinates of vector e_1', e_2' in coordinate system Oe_1e_2 are (a_{11}, a_{21}) and (a_{12}, a_{22}) respectively, and the coordinates of point O' under coordinate system Oe_1e_2 are (a_{13}, a_{23}), then the relationship between $(x, y).(x', y')$ is $\begin{matrix} x' = a_{11}x + a_{12}y + a_{13} \\ y' = a_{21}x + a_{22}y + a_{23} \end{matrix}$ and $\begin{vmatrix} a_{11} & a_{12} \\ a_{21} & a_{22} \end{vmatrix} * 0$, since e_1' is not parallel to e_2', which yields the algebraic representation of the affine transformation.

2.4.2. 2D image deformation algorithm. Let the deformation object be I, the set of user-selected control points be p, and the set of new positions after the points in p are moved be q. The deformation function f should satisfy the following three properties:

1) Interpolation: under the action of function f, the control points p_i mapped to the user-specified position q_i, that is, $f(p_i) = q_i, q_i \in I$;

2) Smoothing: the function f can produce a smooth deformation effect;

3) Constancy: if the control point p_i is the same as its deformed position q_i, then f should be a constant transformation, i.e. $q_i = p_i \Rightarrow f(v) = v$, for every point $v \in I$.

(1) Morphing model. Suppose p is the set of control points on the image and q is the new position of the set of control points p on the deformed image. For any point v on the image, an affine transformation function $l_v(x)$ is desired that minimizes the following expression:

$$\sum_i w_i \, | l_v(p_i) - q_i |^2 \tag{19}$$

where p_i, q_i are all row vectors, w_i satisfy the forms $w_i = \frac{1}{d}$, d_i are the geodesic distances from the control point p_i to the pixel point v within the contour polygon on the image.

Define the transformation: $f(x) = l_v(x)$ to obtain an affine transformation on the whole image.

Since $l_v(x)$ is an affine transformation, $l_v(x)$ contains two parts: a linear transformation matrix M and a flat shift term T, i.e., there are:

$$l_v(x) = xM + T \tag{20}$$

A partial derivation of the variable τ yields $T = q_* - p_* M$, such that expressing T in terms of M eliminates the translation term T. Which:

$$P = \frac{\sum_i w_i p_i}{\sum_i w_i}, q_* = \frac{\sum_i w_i q_i}{\sum_i w_i} \tag{21}$$

By substituting the newly obtained expression for T into Eq. (20), $l_v(x)$ can be rewritten in the form of a linear transformation matrix M only:

$$l_v(x) = (x - p_*)M + q_* \tag{22}$$

In this way, equation (19) can be re-expressed as:

$$\sum_i w_i \,|\, \hat{p}_i M - \hat{q}_i \,|^2 \tag{23}$$

where $\hat{p}_i = p_i - p_*, \hat{q}_i = q_i - q_*$.

The linear transformation matrix that minimizes the above equation can be solved directly using the typical regular equations of Eq. $M = (\sum_i \hat{p}_i^T w_i \hat{p}_i)^{-1} \sum_j \hat{p}_j^T w_i \hat{q}_j$. With an expression for M, it is possible to write a formulaic representation of the transformation function $f(v)$:

$$f(v) = (v - p_*)(\sum_i \hat{p}_i^T w_i \hat{p}_i)^{-1} \sum_j \hat{p}_j^T w_i \hat{q}_j + q_* \tag{24}$$

To minimize expression (19) when v approximates p_i, $l_v(p_i) = q_i$ must hold, and hence the transformation function $f(v)$ is interpolated.

When $p_i = q_i$, then:

$$p_* = \frac{\sum_i w_i p_i}{\sum_i w_i} = \frac{\sum_i w_i q_i}{\sum_i w_i} = q_*, \hat{p}_i = p_i - p_* = q_* - \hat{q}_i \tag{25}$$

The position of pixel v after deformation according to Eq. (24):

$$\begin{aligned} f(v) &= (v - p_*)(\sum_i \hat{p}_i^T w_i \hat{p}_i)^{-1} \sum_j \hat{p}_j^T w_i \hat{q}_j + q_* \\ &= (v - p_*)E_2 + q_* \\ &= v - p_* + q_* = v \end{aligned} \tag{26}$$

E_2 is a two-dimensional unit matrix, so the transformation function $f(v)$ maintains the constant property.

Write equation (24) in the form:

$$f(v) = \sum_j A_j \hat{q}_j + q_* \tag{27}$$

And $A_i = (v - p_*)(\sum_j \hat{p}_i^T w_i \hat{p}_i)^{-1} \hat{p}_j^T w_i$. It can be seen that every variable in the given points v, A_j is precomputable.

(2) Morphing algorithm and its realization. After inputting an image I, the following steps are required to deform it according to the algorithm of this paper:

Outline the object to be deformed, select the set p of control points and the new position q of the deformed control points, and initialize the image pixel matrix PM according to the inside/outside relationship between each point on the image and the outline.

For the points v and control points p_i within each pair S, construct the viewable view $VG(S)$ within the polygon with set $\{v_i \mid v_i \in S\} \cup \{v, p_i\}$ as the vertex and set s as the boundary using the improved rotating tree algorithm, and then compute the geodesic distance d_i from v to p_i using Dijkstra's algorithm, and finally use $w_i = \frac{1}{d}$ as the weight of the control point p_i to the pixel v.

For point v within S the new position after deformation is calculated according to the fast deformation formula (27).

When the new positions of all points within S are calculated, the deformed image is interpolated with a single row and column linear interpolation algorithm.

Plot the output new image. Assuming that the polygon domain S contains n contour vertices and the number of control points selected is m, Fig. 7 depicts the flow of deforming the input image with the algorithm of this paper.

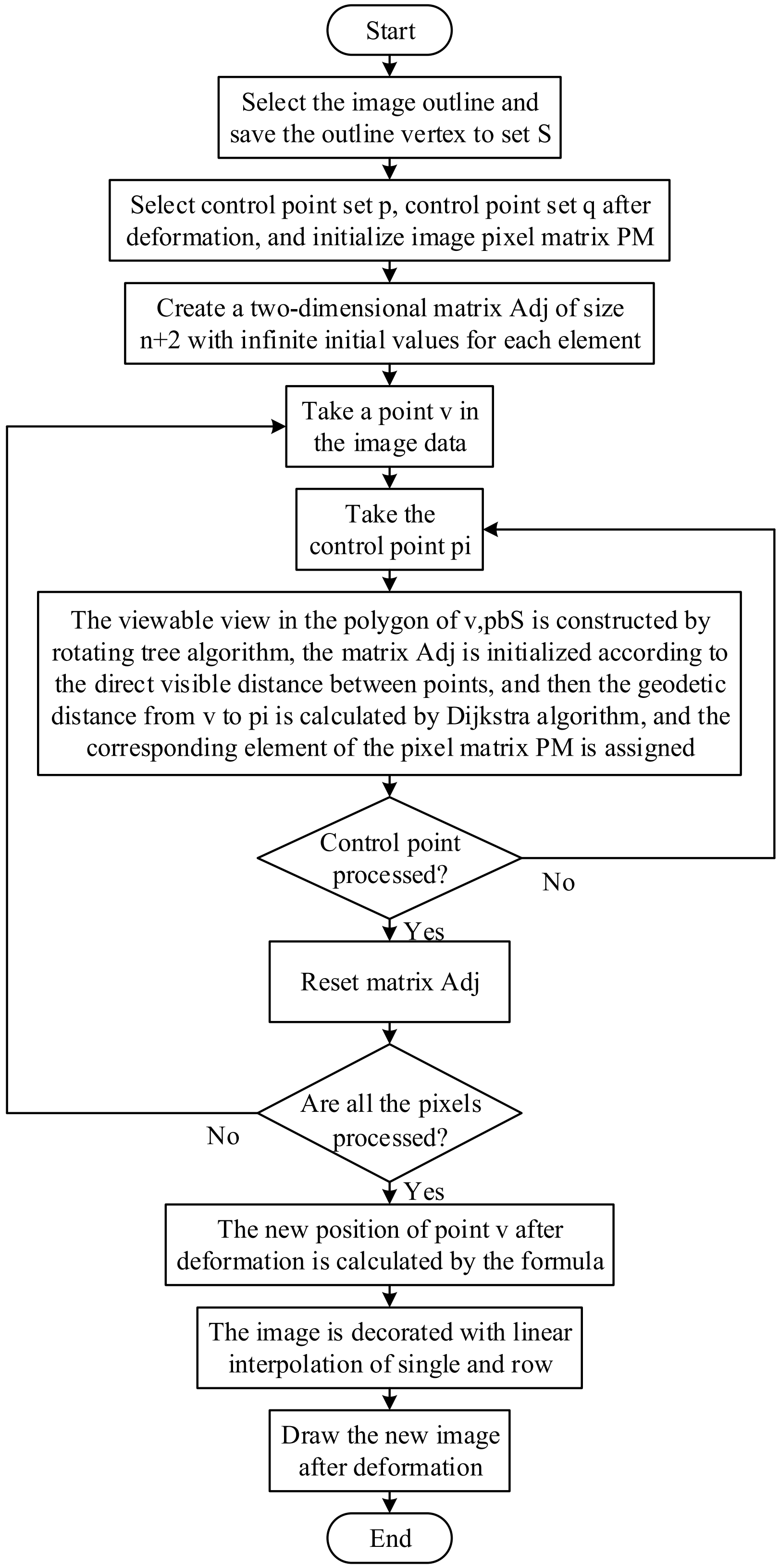

Fig. 7. Flow chart of the deformation algorithm in this paper

3. Geometric deformation results of lacquer decorative pattern under Fourier transform

3.1. Fourier Transform Based Lacquer Decorative Pattern Processing

In the methods of digital image processing, its role is to segment the part of the image that is useful or needs to be used, that is, to divide the picture into a number of small regions of different nature. Some of its applications are edge detection, image binarization etc. Image binarization is the process of changing a color image into a gray and white image, which is based on the principle of changing the gray value of the pixels on the image so that the image will become gray and white. In this paper a color image is read into the program and then this image is binarized and finally the image is processed in programming language. The edge detection method is to detect the gray level of each pixel and then quantize the detected gray level.

3.1.1. Threshold Segmentation. Segment the image into different regions by dividing all the pixels of the picture, each small set obtained will become a subset, each subset will have a corresponding region, different regions have different properties, but the internal properties are the same. The result of threshold segmentation processing is shown in Fig. 8.

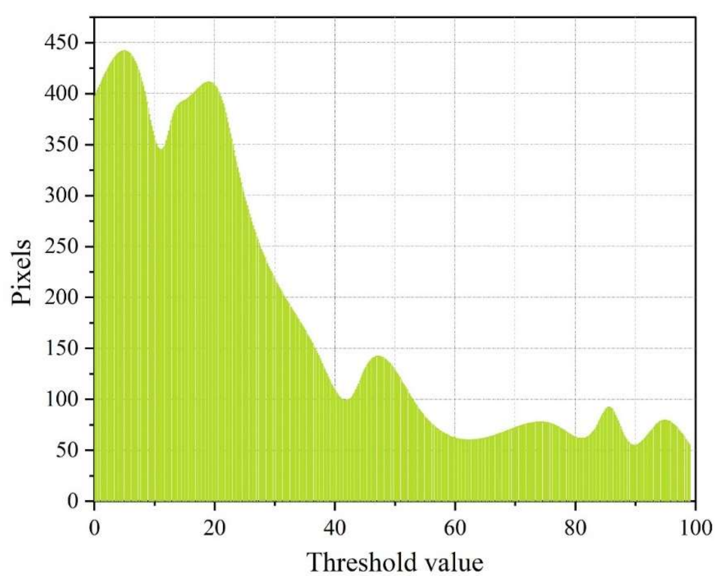

Fig. 8. Threshold partition processing diagram

3.1.2. Brightness. Brightness, i.e. grayscale, can bring out the change of light and darkness of the picture, and the range of change is 0%-100%. The processing results of different brightness are shown in Figure 9, where (a) is 100% brightness and (b) represents 50% brightness. It can be found that the clarity of the picture decreases after turning down the brightness, and the lower the brightness, the more blurred the picture is.

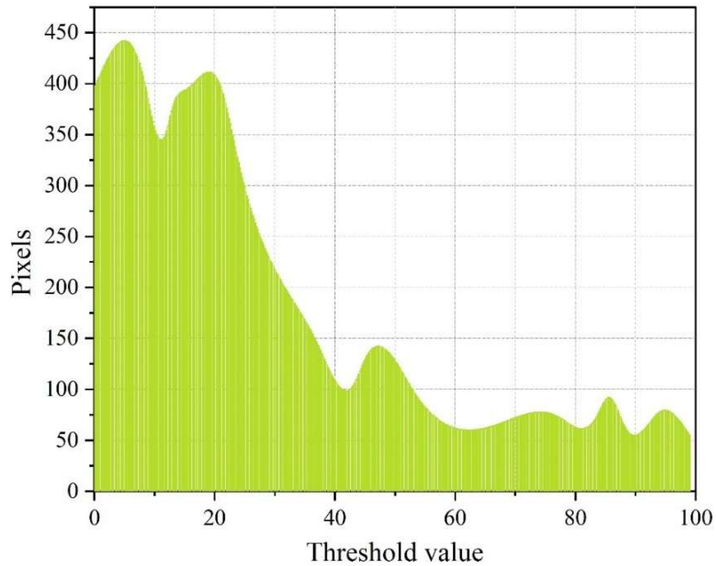

(a)100%

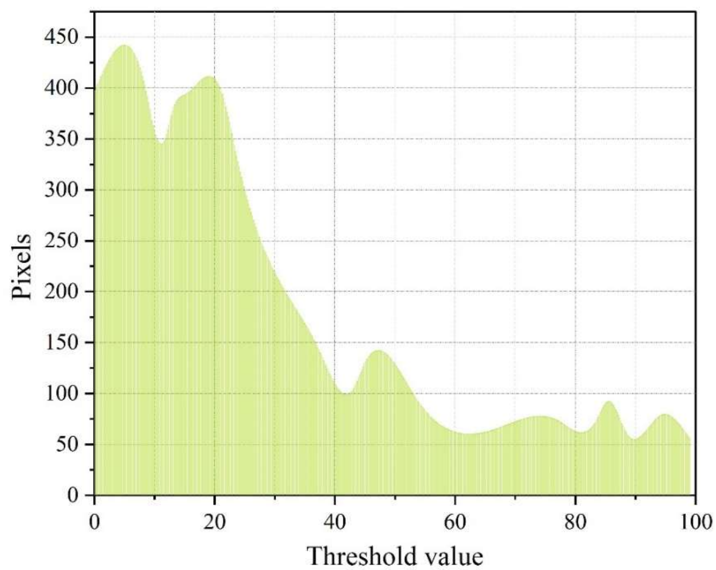

(b)50%

Fig. 9. Different brightness processing results

3.1.3. Contrast. Digital image processing is simply a variety of computer software to perform a variety of image demonstration, MATLAB can be visualized image demonstration. Therefore, this paper uses the GUI platform in MATLAB to carry out some basic processing of images, such as image cropping, displaying the boundary map of the image, adjusting the brightness, contrast adjustment, cropping and intercepting, and displaying the effect of image negatives and other operations. After that, through the analysis algorithm in this paper, the method of improving the pattern design in lacquer decorative design and the geometric deformation of the image is improved, and the processing effect is demonstrated through examples.

The result of image contrast adjustment is shown in Fig. 10, (a)~(c) represent the original image, contrast default image and 2D true color transformed image respectively. Adjusting the contrast means changing the ratio of black and white in the image, and the larger the ratio is, the greater the change in the color gradient level of the image will be, so that the image becomes richer in color. Processing results found that, compared with the original image, with the adjustment of contrast, the color in the image is found to be changed from the original green to yellow-green color. The image processed by the 2D True Color Transformation technique in this paper shows richer color variations with yellow and green showing different shades of color and richer color variations.

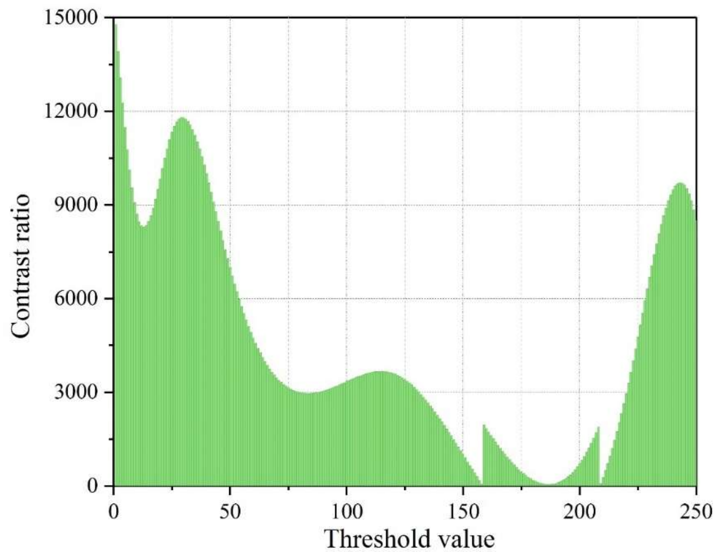

(a)Original image

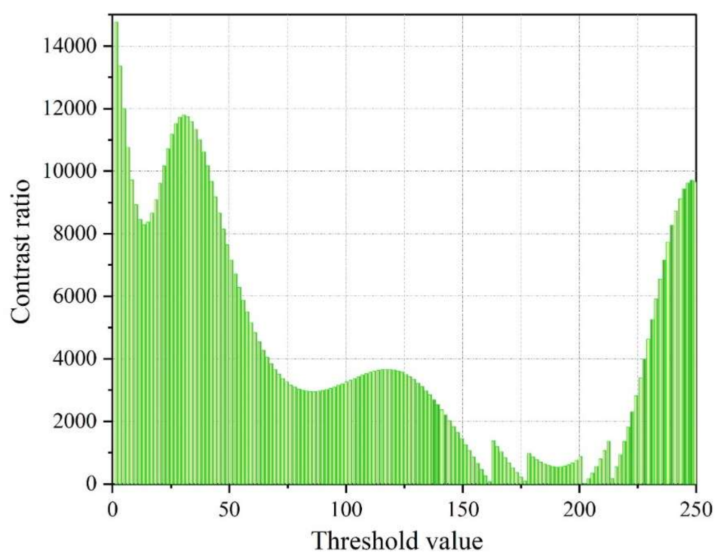

(b)Contrast the default image

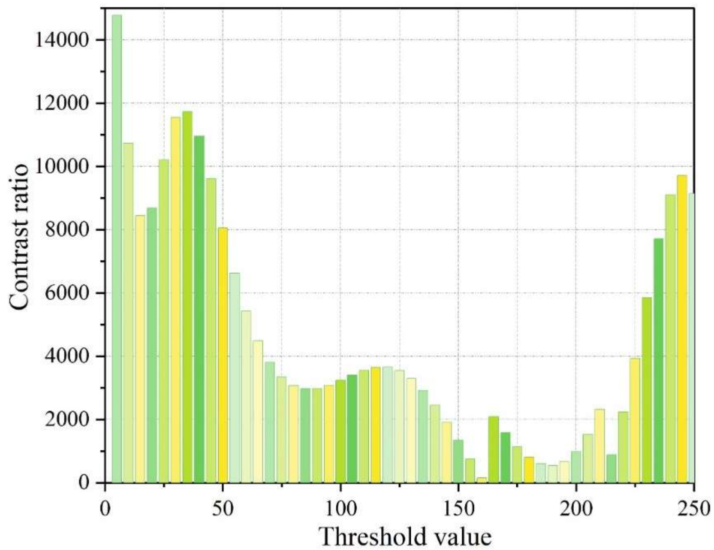

(c)2D real color transform image

Fig. 10. Image contrast adjustment results

3.2. Lacquer decorative design pattern color analysis

In this paper, several scene patterns of lacquer decoration design are collected, and the final geometric deformation pattern is obtained by the 2D image deformation algorithm in this paper. The original size of the image is 524×524, and the generated geometric deformation pattern is also 524×524, and the size of the geometric deformation pattern "dot matrix" block is 10×10, which is somewhat reduced here. The three-dimensional color statistics of the figure, and then use the fast method to select one of the four larger peaks M1, M2, M3, M4, different values of B, three-dimensional color statistics as shown in Figure 11, (a) ~ (d) represent B = 38, B = 104, B = 256 and B = 418, respectively.

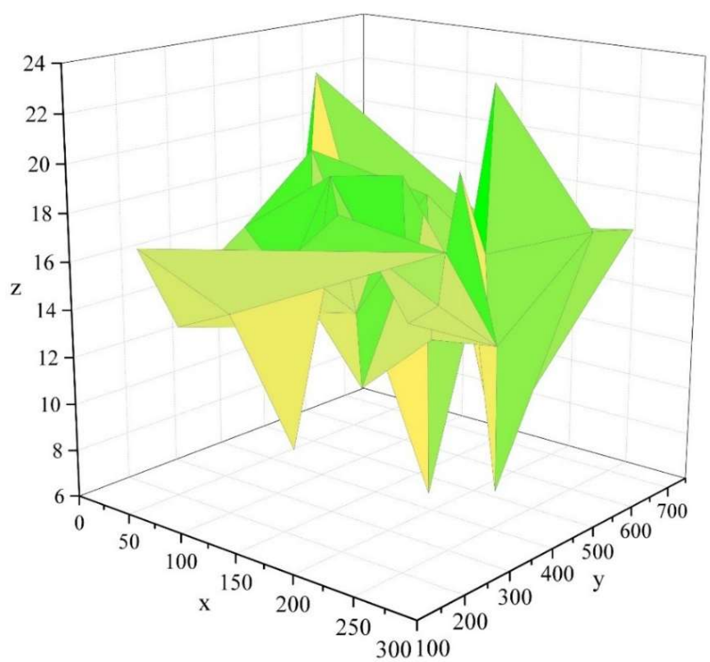

(a)B=38

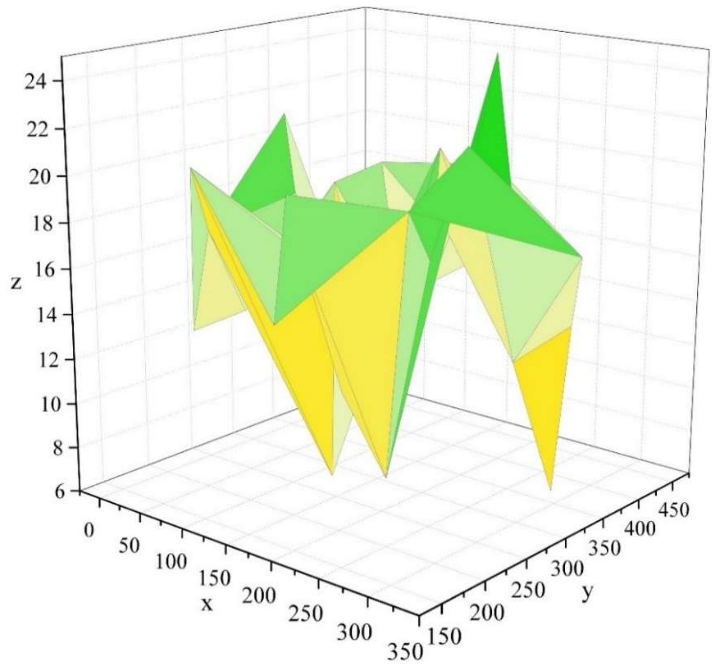
24
22
20
18
16
14
12
10
8
6
z
0
50
100
150
200
250
300
350
x
150
200
250
300
350
400
450
y

(b)B=104

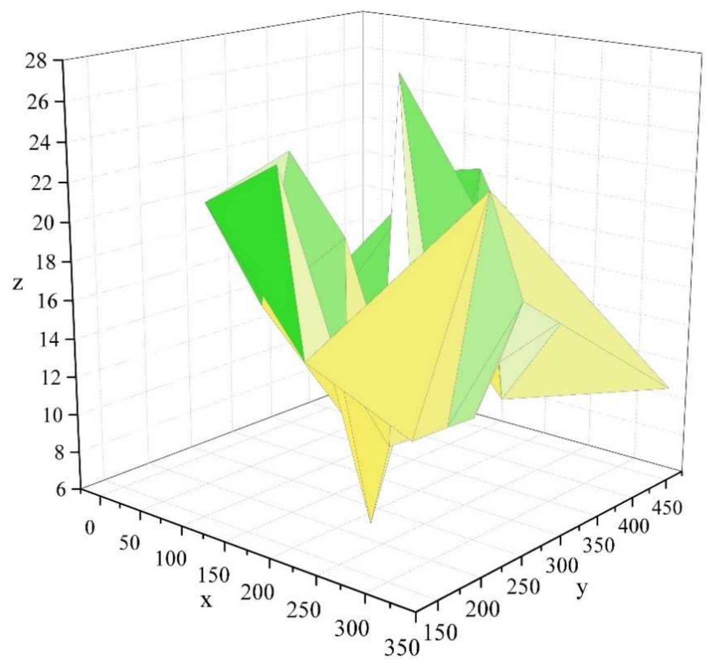
28
26
24
22
20
18
16
14
12
10
8
6
z
0
50
100
150
200
250
300
350
x
150
200
250
300
350
400
450
y

(c)B=256

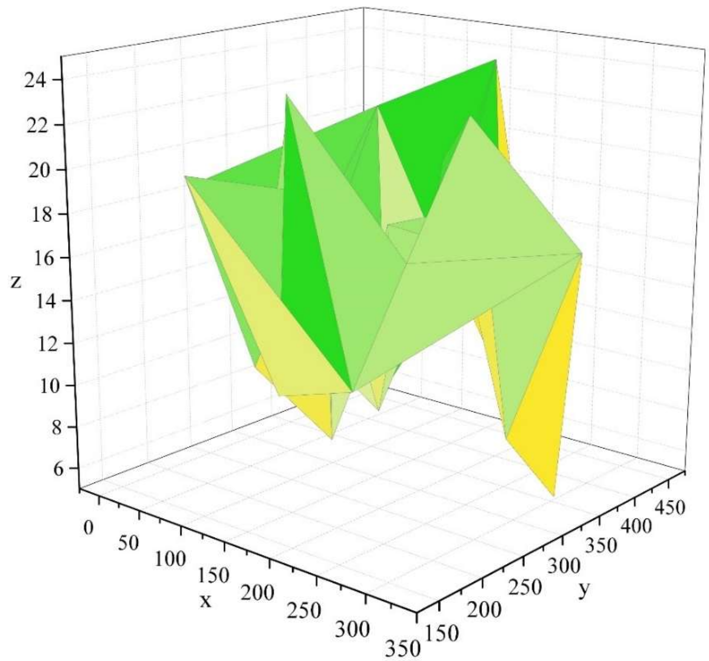

(d)B=418

Fig. 11. The three-dimensional color statistics of different b values

The R and G components of the pixel values constitute the X-Y plane in the spatial Cartesian coordinate system, and the different four statistical diagrams represent the statistics of the number of pixels at different B values, respectively. The fast algorithm of neighborhood removal is used to select the maximum point of the image at first, and then the neighborhood is removed to select the maximum point in the remaining neighborhood, and in turn, four times, and the final extracted dominant color values of the original image are shown in Table 2. The experimental results found that the optimal component values of blue, green and red colors corresponding to the No. 1 pattern obtained in this paper are 418, 256 and 256, respectively; the No. 2 pattern is 38, 100 and 57; the No. 3 and No. 4 are 104, 87, 63 and 256, 405 and 117, respectively.

Table 2. The primary color value of the original image

Pattern number	B	G	R
1	418	256	256
2	38	100	57
3	104	87	63
4	256	405	117

3.3. Three-dimensional imaging simulation experiment and result analysis

Three-dimensional imaging experiments of Fourier transform-based patterns in lacquerware decorative designs were carried out using the two methods developed and the two-dimensional Fourier transform method based on the positive stripe pattern. The 3D imaging results of the lacquerware decorative designs using different methods are shown in Fig. 12, (a) ~ (c) are the Fourier transform of the pattern under the orthostripe pattern Fourier transform, the diagonal stripe pattern Fourier transform and the geodesic distance deformation algorithm based on the Fourier transform, respectively. The coordinates (x, y, z) in the figure represent the spatial 3D coordinates (x,y,z).

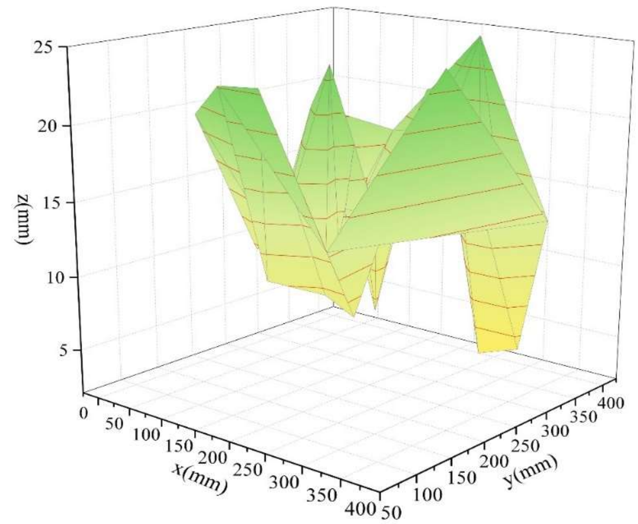

(a)Fourier transform of the positive fringe pattern

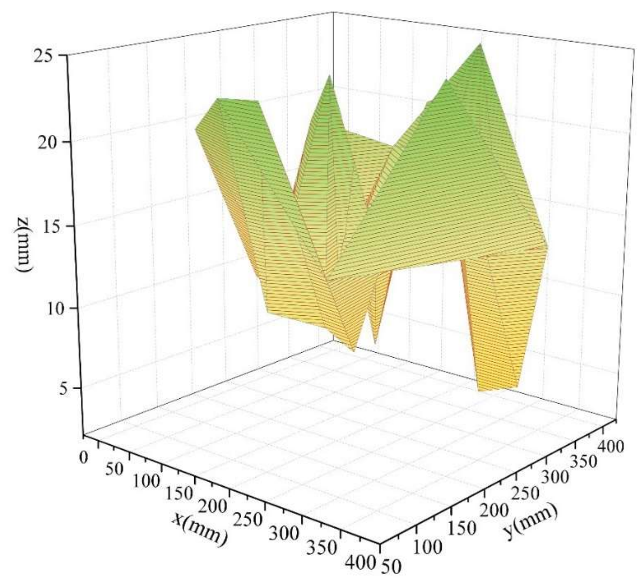

(b)Diagonal stripe pattern Fourier transform

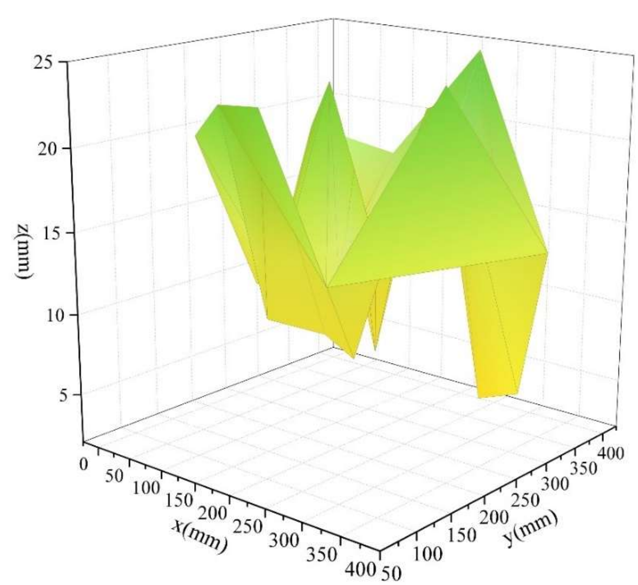

(c)The distance deformation algorithm under the Fourier transform

Fig. 12. 3D imaging of decorative patterns of lacquer in different methods

In order to quantitatively evaluate the measurement accuracy of 3D imaging methods [20] targeting geometric patterns, mathematical expressions capable of expressing the relationship between the depth values of geometric patterns and the coordinates of image pixels were established:

$$\begin{aligned}&(a^2+c^2+a^2c^2)\times Z_r(x_0,y_0)^2\\&-(2bc^2+2Ca^2)\times Z_r(x_0,y_0)\\&+b^2c^2+a^2C^2-r^2a^2c^2=0\end{aligned} \tag{28}$$

$$a=\tan\left\{\beta_0-\arctan\left[(n_0/2-x_0)d_{x_0}/f_0\right]\right\} \tag{29}$$

$$b=C-aB \tag{30}$$

$$\begin{aligned}&c=\sqrt{[(n_0/2-x_0)d_{x_0}+f_0^2]}\\&\times\sin\left\{\beta_0-a\tan\left[(n_0/2-x_0)d_{x_0}/f_0\right]\right\}/\left[-d_{y_0}[(m_0/2-y_0)\right]\end{aligned} \tag{31}$$

where: $tan()$ is the tangent function, $a\tan()$ is the arctangent function; (x_0,y_0) is the pixel coordinate of the image; r is the radius of the geometric pattern; C is the distance between the intersection of the optical axis of the projector and the optical axis of the camera and the center of the projector lens; B is the distance between the center of the projector lens and the center of the camera lens; β_0 is the angle between the main optical axis of the camera and the OX axis; f_0 is the focal length of the camera lens; d_{x_0} and d_{y0} are the individual pixel sizes along the x_0-axis and y_0-axis directions on the camera imaging surface, respectively; n_0 and m_0 are the image plane heights (number of pixels) of the camera along the x_0th and y_0th axes, respectively; $Z_r(x_0,y_0)$ is the depth value of the geometric pattern corresponding to the image coordinate (x_0,y_0), and this value is used as the true value of the agreed depth of the geometric pattern, and is used to quantitatively evaluate the measurement accuracy of the three-dimensional imaging method. This shows the depth imaging error distribution at a change in slope of the measured surface $\pm 30°$, where coordinate (j,i) represents the image pixel coordinate (x_0,y_0).

The 3D imaging results of geometric images using different methods are shown in Fig. 13, and (a) ~ (c) are the pattern Fourier transforms under the positive stripe pattern Fourier transform, the diagonal stripe pattern Fourier transform, and the geodetic distance deformation algorithm based on the Fourier transform, respectively. The geometric pattern depth imaging errors using different methods are shown in Table 3. Compared with the 3D imaging method based on the positive stripe pattern Fourier transform, the average absolute error and the root mean square error of the geometric pattern depth using the 3D imaging method based on the diagonal stripe pattern Fourier transform and the geodetic distance deformation algorithm based on the Fourier transform are both significantly reduced, and the maximum absolute error of this paper's method is also significantly reduced, and only the maximum absolute error of the 3D imaging method based on the diagonal stripe pattern Fourier transform is slightly larger. In contrast, the depth imaging error of this paper's method is minimized, which indicates that the two methods developed are more advantageous over a depth variation range of up to 20 mm. Therefore, with depth and slope variations limited to 20 mm and 63°, the diagonal stripe pattern method and the method in this paper are clearly superior to the orthostripe pattern method.

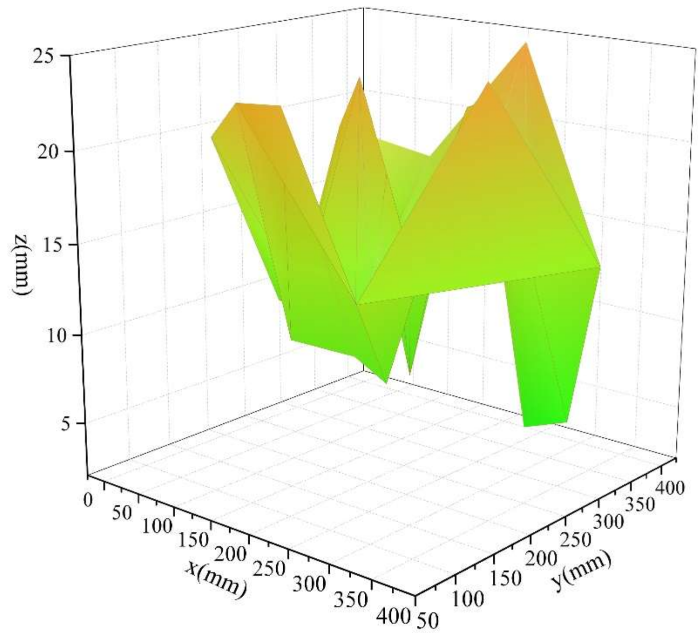

(a) Fourier transform of the positive fringe pattern

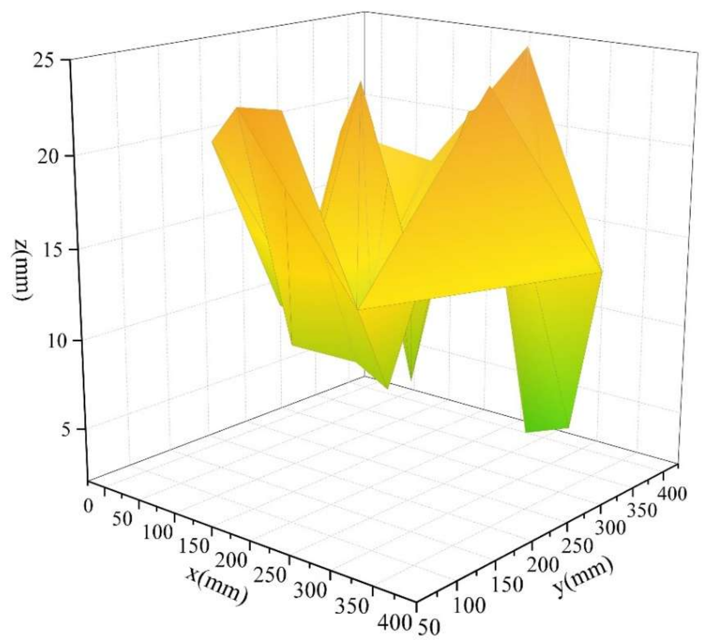

(b) Diagonal stripe pattern Fourier transform

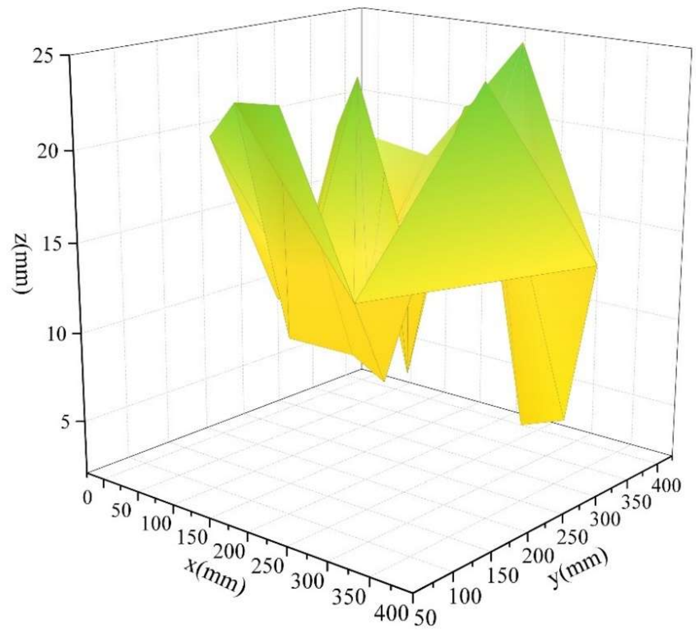

(c) The distance deformation algorithm under the Fourier transform

Fig. 13. 3D imaging of geometric images with different methods

Table 3. The effect of the crown depth imaging error of different methods

Error	The normal stripe pattern Fourier transform	The Fourier transform of the diagonal pattern	Improvement method
Maximum absolute error (mm)	0.3748	0.3942	0.2737
Average absolute error (mm)	0.1176	0.0855	0.0134
Mean square root error (mm)	0.1422	0.1036	0.0957

4. Conclusion

This study focuses on the field of lacquer decoration design, proposes the geometric deformation algorithm of pattern based on geodesic distance, segments the original image and extracts the color, and analyzes the three-dimensional imaging results of lacquer decoration pattern under different methods, expecting to enhance the artistic effect and cultural connotation of lacquer decoration through geometric deformation. The main conclusions are as follows:

1) In this paper, a color image is read in the MATLAB program, and then this image is binarized, and finally the image is processed by the programming language, and then the detected grayscale is quantized. The threshold distribution, brightness and contrast of the key parts of the image after segmentation are finally obtained.

2) In this paper, we use a fast algorithm to select the largest extreme value point among them, and take the block as a unit, according to the Euclidean distance between the average value in the block and the extreme value point, select the appropriate main color, fill the color in the block, and get the final lacquer decorative design geometric pattern.

3) In the three-dimensional imaging simulation experiments, the two-dimensional Fourier transform three-dimensional imaging method based on the positive stripe pattern, the two-dimensional Fourier transform three-dimensional imaging method based on the diagonal stripe pattern, and the geodesic distance deformation algorithm based on the Fourier transform proposed in this paper are used to carry out three-dimensional imaging simulation experiments on the typical planar surface and

geometric patterns with different slopes, respectively. The feasibility of the three-dimensional coordinate measurement model of the Fourier transform-based geodesic distance deformation algorithm constructed in this paper is proved.

References

[1] Körber, U., Schilling, M. R., Dias, C. B., & Dias, L. (2016). Simplified Chinese lacquer techniques and Nanban style decoration on Luso-Asian objects from the late sixteenth or early seventeenth centuries. Studies in Conservation, 61(sup3), 68-84.

[2] Wang, M. (2017, February). Innovation and development of arts and crafts in lacquer art research. In 2017 International Conference on Humanities Science, Management and Education Technology (HSMET 2017) (pp. 786-789). Atlantis Press.

[3] Cheng, L. (2023). Research on the Discrepancy and blending of Lacquer Ceramic Art. Journal of Education, Humanities and Social Sciences, 21, 280-288.

[4] Shen, J. S., Xiao, Y. M., & Lin, R. (2022, June). A Study on the Innovation of Traditional Lacquer Art: The Creation of Paper-Based Lacquer Paintings as an Example. In International Conference on Human-Computer Interaction (pp. 255-267). Cham: Springer International Publishing.

[5] Xiao, Y. M., Shen, J. S., & Lin, C. L. (2024). Exploring on the Extraction of Attributes of Lacquer Art Fashion Products. Creative Education, 15(04), 617-642.

[6] Lin, X. (2019, January). Lacquer Decoration Technology in Bag Design. In 2nd International Conference on Social Science, Public Health and Education (SSPHE 2018) (pp. 355-358). Atlantis Press.

[7] Jin, Y. (2024). Research on the Application of Lacquer Painting Techniques in Modern Handicrafts. Frontiers in Art Research, 6(9).

[8] Bai, J., Sun, Y., Kim, W. S., Ro, H. S., & Kim, S. M. (2019). Chinese Porcelain Lacquer Painting Art: Primary Analysis on Convergence of Porcelain Decoration and Raw Lacquer. Journal of Digital Convergence, 17(10), 405-410.

[9] Yong, L. (2019). The Charm of Skills-The Exploration of the Modern Lacquerware. Academic Journal of Humanities & Social Sciences, 2(5), 74-81.

[10] Tamburini, D., Kotonski, V., Lluveras-Tenorio, A., Colombini, M. P., & Green, A. (2019). The evolution of the materials used in the yun technique for the decoration of Burmese objects: lacquer, binding media and pigments. Heritage Science, 7, 1-23.

[11] Sun, F., & Shu, W. (2020). Research on the Innovative Approach of Intergrowth of Xipi Lacquer Art in Huizhou and Modern Product Design. In E3S Web of Conferences (Vol. 179, p. 02069). E3S Web of Conferences.

[12] Shen, R. (2023). Research on the Design of Beijing Carved Lacquerware Derivatives from the Perspective of Experience Design. Journal of Research in Social Science and Humanities, 2(5), 19-24.

[13] Quanwei, M. A. (2023). THE APPLICATION OF TRADITIONAL PATTERN DESIGN OF LACQUERWARE UNEARTHED IN NANCHANG HAIHUNHOU IN CULTURAL AND CREATIVE PRODUCTS. Procedia of Multidisciplinary Research, 1(9), 6-6.

[14] Barkeshli, M., Rostami, M., & Zekrgoo, S. (2023). Characteristics of Traditional Persian Lacquered Bindings and Specific Deterioration Issues. Restaurator. International Journal for the Preservation of Library and Archival Material, 44(4), 295-343.

[15] Yao, J. (2024). Process design and cultural interaction of thai export lacquerware from a crosscultural perspective. Arts Educa, 39.

[16] Lin, X. (2024). The spirit of" Art Deco movement" in Fuzhou area of China is integrated into lacquer accessories. International Journal of Multidisciplinary in Management and Tourism, 8(1).

[17] David J Degnan,Daniel M Claborne,Amanda M White,Sarah M Akers,Natalie M Winans,Yuri E Corilo... & Lisa M Bramer. (2025). FREDA: A Web Application for the Processing, Analysis, and Visualization of Fourier-Transform Mass Spectrometry Data.. Rapid communications in mass spectrometry : RCM(7),e9980.

[18] Lina Zhang & Yi Wan. (2024). Color-to-gray image conversion using salient colors and radial basis functions. Journal of Electronic Imaging(1),013047-013047.

[19] Yi Bowen,Li Rui,Li Weidong,Wang Xiaosun,Wu Shijing & Huang Nuodi. (2023). Adaptive milling for contours on deformed surface based on on-machine measurement and optimized parallel projection. The International Journal of Advanced Manufacturing Technology(1-2),443-452.

[20] Yun Taek Shim,Ye Hwon Jeong,Nahyun Aum,Hong Il Ha,Minsung Choi,Jin Young Hyun... & Yi Suk Kim. (2024). A new metric method for sex estimation using three-dimensional imaging of the nuchal crest.. Anatomy & cell biology